

# Dielectric Spectroscopy of Aqueous Solutions of KCl and CsCl

Ting Chen and Glenn Hefter\*

Chemistry-DSE, Murdoch University, Murdoch, W.A. 6150, Australia

Richard Buchner\*

Institut für Physikalische und Theoretische Chemie, Universität Regensburg, D-93040 Regensburg, Germany

Received: July 2, 2002; In Final Form: March 4, 2003

Results of a dielectric relaxation study of the aqueous solutions of KCl and CsCl at 25 °C are reported using measurements with a vector network analyzer ( $0.2 \leq \nu/\text{GHz} \leq 20$ ) and with waveguide interferometers ( $27 \leq \nu/\text{GHz} \leq 89$ ). Similar to previously reported data for NaCl, the spectra of both salts are well fitted by a Cole–Cole equation, although a double-Debye model is competitive at intermediate CsCl concentrations. The impact of the solute on the water structure, reflected in a decrease in the bulk-water relaxation time with rising electrolyte concentration, decreases in the sequence NaCl > KCl > CsCl and appears to be proportional to the surface-charge density of the cation. The interactions of  $\text{K}^+$  and  $\text{Cs}^+$  with their hydration shells are too weak to cause irrotational bonding of  $\text{H}_2\text{O}$  molecules. It is argued that CsCl exhibits weak ion pairing, although the data are not sufficiently accurate to determine the extent of association and the nature of the ion pair formed.

## 1. Introduction

All of the alkali metal chlorides are highly soluble in water, producing strong electrolyte solutions that have been intensively investigated by a great variety of experimental techniques and also by computer simulations.<sup>1–4</sup> These solutions form a particularly useful series in which the cation size varies systematically and, as such, they have also been widely employed to test theories of ionic solutions. The alkali metal chlorides have also been used extensively as “background” electrolytes for controlling ionic strength in the study of complexation and other equilibria.<sup>5–7</sup>

Most of the physicochemical and thermodynamic properties of aqueous alkali metal chloride solutions, such as densities, conductivities, activities, and so on, have been well characterized, often up to saturation concentrations.<sup>8–10</sup> Nevertheless, many uncertainties remain about the nature of these supposedly “simple” strong electrolyte solutions. To take just one example, there are significant discrepancies between the coordination numbers of the cations, as estimated by scattering measurements and computer simulations on one hand, and the hydration numbers as determined by many other techniques.<sup>11</sup>

Dielectric relaxation spectroscopy (DRS),<sup>12,13</sup> which probes the interaction of a sample with an applied electromagnetic field, expressed by the complex permittivity  $\hat{\epsilon}(\nu) = \epsilon'(\nu) - i\epsilon''(\nu)$  as a function of the frequency ( $\nu$ ) of that field, is a potentially powerful technique for studying the solvation and dynamic characteristics of electrolyte solutions.<sup>14–16</sup> Surprisingly few DRS investigations have been reported for alkali metal chloride solutions, mostly over limited ranges of concentration and/or frequency.<sup>17</sup> Furthermore, almost all of these studies are rather old and, because of the technological limitations of the times,<sup>18</sup> the data obtained were generally of low accuracy and limited usefulness.

Recently, some of us have published<sup>19</sup> a detailed reinvestigation of the NaCl(aq) solutions using state-of-the-art instrumentation based on a vector network analyzer (VNA) over the frequency range of  $0.2 \leq \nu/\text{GHz} \leq 20$  and at concentrations up to  $5 \text{ mol kg}^{-1}$ . That study enabled the determination of effective solvation numbers for the dissolved ions and provided insight into the dynamical behavior of NaCl(aq) solutions. The present paper reports analogous measurements on KCl(aq) and CsCl(aq) solutions at 25 °C over as wide a concentration range as practical. This investigation has been stimulated in part by recent observations suggesting that CsCl may be problematic as a background electrolyte.<sup>6,7</sup> By combining VNA and interferometric measurements, it has been possible to cover frequencies up to 89 GHz.

## 2. Experimental Section

Target solutions were prepared volumetrically using calibrated A-grade glassware without buoyancy corrections. All concentrations are expressed in molarity. The salts KCl (Ajax Chemicals, Australia, AR grade, 99.8% purity) and CsCl (BDH, UK, AR grade, 99.9%) were dried at 50 °C for ~4 h under vacuum (~1 kPa) and were stored in a vacuum desiccator. Densities required for the calculation of water concentrations were obtained from the ELDAR database,<sup>20</sup> as were the conductivities of KCl(aq) and CsCl(aq), which were used for kinetic depolarization corrections.

Dielectric spectra at  $\nu_{\text{min}} \leq \nu \leq 20 \text{ GHz}$  were obtained at Murdoch University using a Hewlett-Packard model 85070M dielectric probe system based on an HP 8720D VNA as described previously.<sup>19</sup> Temperature was controlled by a Hetofrig (Denmark) circulator-thermostat to  $\leq 0.02 \text{ }^\circ\text{C}$  with an accuracy of better than  $0.05 \text{ }^\circ\text{C}$ . The value of the minimum frequency of investigation,  $\nu_{\text{min}}$ , was determined by the conductivity contribution to the loss spectrum (see below). As such, it varied with concentration but was typically in the range of

\* To whom correspondence should be addressed. E-mail: hefter@chem.murdoch.edu.au. Richard.Buchner@chemie.uni-regensburg.de.

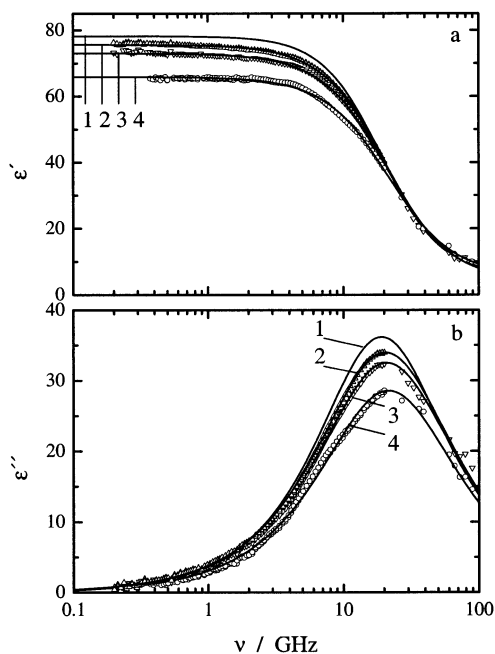


**Figure 1.** Dielectric dispersion,  $\epsilon'(\nu)$  (a), and loss,  $\epsilon''(\nu)$  (b), spectra of water (1, ref 23) and aqueous KCl solutions of  $c = 0.15$  M (2), 0.60 M (3), and 1.42 M (4) at 25 °C. Solid lines for curves 2–4 represent the fits with the CC model.

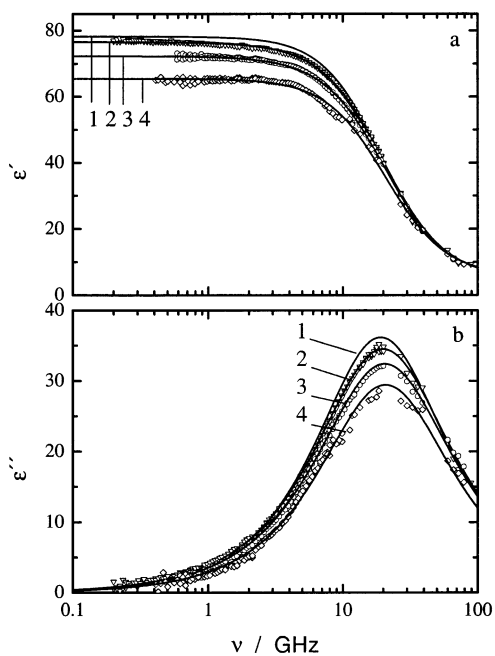


**Figure 2.** Dielectric dispersion,  $\epsilon'(\nu)$  (a), and loss,  $\epsilon''(\nu)$  (b), spectra of water (1, ref 23) and aqueous CsCl solutions of  $c = 0.25$  M (2), 0.80 M (3), and 1.76 M (4) at 25 °C. Solid lines for curves 2–4 represent the fits with the CC model.

(0.2 to 0.5) GHz. All VNA spectra were recorded using at least two independent calibrations, with air, water, and mercury as the references. Higher-frequency data for selected solutions were recorded at Regensburg using two interferometers: A-band ( $27 \leq \nu/\text{GHz} \leq 39$ ) and E-band ( $60 \leq \nu/\text{GHz} \leq 89$ ). The operation of these instruments is described in detail elsewhere.<sup>15,21</sup> Temperature control and accuracy were similar to those at Murdoch. Typical spectra and corresponding fits (see below) are shown in Figures 1 and 2; all data are tabulated in the Supporting Information.

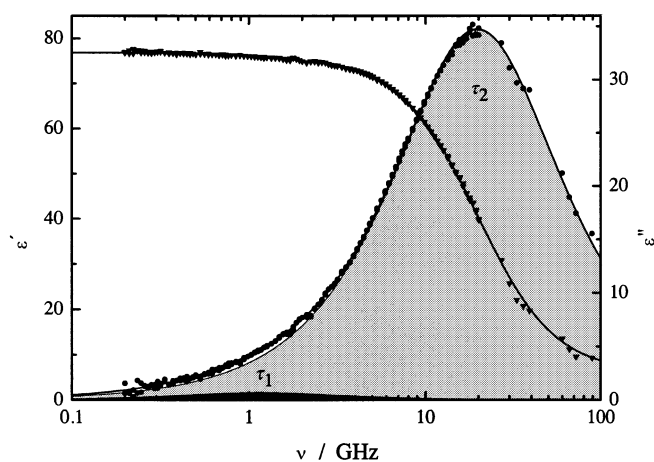


**Figure 3.** Dielectric dispersion,  $\epsilon'(\nu)$  ( $\blacktriangledown$ ), and loss,  $\epsilon''(\nu)$  ( $\bullet$ ), spectra of a 0.25 M aqueous CsCl solution fitted with the 2D model (—). The shaded areas indicate the contributions of relaxation processes 1 and 2 to  $\epsilon''$ .

### 3. Data Analysis

For an electrolyte solution of conductivity  $\kappa$ , DRS determines the relative dielectric permittivity,  $\epsilon'(\nu)$ , and the total loss,  $\eta''(\nu)$ , which is related to the dielectric loss,  $\epsilon''(\nu)$ , as

$$\eta''(\nu) = \epsilon''(\nu) + \frac{\kappa}{2\pi\nu\epsilon_0} \quad (1)$$

where  $\epsilon_0$  is the permittivity of a vacuum. To obtain  $\epsilon''(\nu)$ , each VNA spectrum was analyzed separately to determine the slightly calibration-dependent effective conductivity,  $\kappa_e$ , at each concentration. As previously reported,<sup>22</sup> the effective conductivity was obtained by fitting the experimental total loss curve to eq 1. The  $\kappa_e$  values so obtained are generally 1–2% smaller than conventional (low-frequency) conductivities<sup>20</sup> with slightly larger deviations at high concentrations. For the correction of the interferometer data,  $\kappa$  values from the literature were used.<sup>20</sup> Provided sufficient reproducibility was obtained for  $\kappa_e$  ( $\pm 2\%$ ), at least two VNA spectra and, when determined, the interferometer data were combined after a correction of  $\eta''$  for the ohmic loss,  $\kappa/(2\pi\nu\epsilon_0)$ . As can be seen from Figures 1–3, there is in general a seamless fit between the low- and high-frequency data, although, as is usually observed for electrolyte solutions, the noise increases with increasing concentration because of the increasing conductivity contribution.<sup>19,22</sup>

The combined  $\hat{\epsilon}(\nu)$  data were fit to various conceivable relaxation models. It was found that, for KCl solutions,  $\hat{\epsilon}(\nu)$  was always best fit by a single Cole–Cole equation (the CC model):

$$\hat{\epsilon}(\nu) = \frac{\epsilon - \epsilon_\infty}{1 + (i2\pi\nu\tau)^{1-\alpha}} + \epsilon_\infty \quad (2)$$

where  $\epsilon$  is the “static” permittivity,  $\epsilon_\infty$  is the “infinite-frequency” permittivity of the sample,  $\tau$  is its principal relaxation time, and  $0 \leq \alpha < 1$  is a measure of the width of the symmetric distribution of relaxation times.<sup>12</sup> Equation 2 also gives the best fit for the most dilute and the concentrated CsCl solutions as well as acceptable fits at intermediate  $c$ . The parameters obtained for both KCl and CsCl are summarized in Table 1, together with the average of  $\kappa_e$  and the variance of the fit  $s^2$ . To minimize the number of adjustable parameters, for the spectra of samples with VNA data only,  $\tau$  was fixed to the value interpolated with

**TABLE 1: Concentration  $c$ , Average Effective Conductivity  $\kappa_e$ , DR Parameters  $\epsilon$ ,  $\tau$ ,  $\alpha$ , and  $\epsilon_\infty$ , and the Variance  $s^2$  of the Fit of the CC Model to  $\hat{\epsilon}(\nu)$  for Aqueous Solutions of KCl and CsCl at 25 °C<sup>a</sup>**

$c$	$\kappa_e$	$\epsilon$	$\tau$	$\alpha$	$\epsilon_\infty$	$s^2$
KCl						
0.0519	0.678	77.73	8.24F	0.002	6.35	0.02
0.1030	1.30	77.41	8.17F	0.011	5.80	0.04
0.1504	1.85	76.94	8.13	0.013	5.21	0.14
0.2497	2.99	76.15	7.99F	0.025	5.04	0.07
0.3153	3.70	75.63	7.92F	0.028	4.85	0.07
0.4408	5.06	74.52	7.80F	0.034	4.47	0.06
0.6008	6.78	72.97	7.71	0.034	4.31	0.14
0.7931	8.79	71.23	7.57F	0.036	4.79	0.10
1.104	11.8	68.20	7.46F	0.036	5.08	0.11
1.423	15.0	65.93	7.41	0.034	5.66	0.22
CsCl						
0.0504	0.673	78.05	8.27F	0.008	6.12	0.04
0.0994	1.29	77.67	8.22F	0.017	5.88	0.05
0.1500	1.88	77.30	8.17F	0.017	5.74	0.08
0.2499	3.03	76.54	7.99	0.025	4.73	0.14
0.4016	4.71	75.48	7.97F	0.030	5.33	0.08
0.6009	6.86	73.87	7.85F	0.032	5.34	0.10
0.7964	8.90	72.33	7.70	0.030	4.32	0.15
1.106	11.9	70.23	7.68F	0.038	5.65	0.16
1.506	16.1	67.20	7.67F	0.028	6.33	0.35
1.760	18.6	65.49	7.66	0.009	5.77	0.48

<sup>a</sup> Parameter values followed by "F" were not adjusted during the fit. Units:  $c$  in M;  $\kappa_e$  in  $\Omega^{-1} \text{ m}^{-1}$ ;  $\tau$  in  $10^{-12}$  s.

**TABLE 2: Concentration  $c$ , DR Parameters  $\epsilon$ ,  $\tau_1$ ,  $\epsilon_2$ ,  $\tau_2$ , and  $\epsilon_\infty$ , and Variance  $s^2$  of the Fit of the 2D Model to  $\hat{\epsilon}(\nu)$  for Dilute Aqueous Solutions of CsCl at 25 °C<sup>a</sup>**

$c$	$\epsilon$	$\tau_1$	$\epsilon_2$	$\tau_2$	$\epsilon_\infty$	$s^2$
0.0994	77.89	143	76.90	8.22F	6.44	0.03
0.1500	77.66	169	76.52	8.17F	6.33	0.04
0.2499	76.88	140	75.46	8.08	6.10	0.09
0.4016	75.67	100	74.05	7.97F	6.38	0.06
0.6009	73.99	120F	72.68	7.85F	5.97	0.14

<sup>a</sup> Parameter values followed by "F" were not adjusted during the fit. Units:  $c$  in M;  $\tau_1, \tau_2$  in  $10^{-12}$  s.

the help of eq 4 (see below) from the samples where  $\hat{\epsilon}(\nu)$  covered the range of  $\nu_{\min} \leq \nu \leq 89$  GHz.

It appeared that, for CsCl solutions at  $0.1 \leq c/M \leq 0.6$ , a fit to a sum of two Debye equations (the 2D model)

$$\hat{\epsilon}(\nu) = \frac{\epsilon - \epsilon_2}{1 + i2\pi\nu\tau_1} + \frac{\epsilon_2 - \epsilon_\infty}{1 + i2\pi\nu\tau_2} + \epsilon_\infty \quad (3)$$

gave a similar or even better variance  $s^2$ , as exemplified by Figure 3. Because  $\tau_2(2D) = \tau(CC)$  for the VNA-only spectra ( $\nu_{\min} \leq \nu \leq 20$  GHz), this suggests that, at least for CsCl, the parameter  $\alpha > 0$  of the CC model is a reflection of the small additional relaxation process that appears at low frequencies and is described by the amplitude  $S_1 = \epsilon - \epsilon_2$  and the relaxation time  $\tau_1 \approx 140$  ps with the 2D model. The obtained fitting parameters are summarized in Table 2.

## 4. Results and Discussion

**4.1. General Comments.** As expected,<sup>23</sup> the major feature of the spectra for both solutions is a process centered on  $\sim 8$  ps ( $\sim 20$  GHz) corresponding to the cooperative relaxation ( $\tau_b$ ) of the bulk-water molecules. In addition, there is a high-frequency process at  $\tau_f \approx 1$  ps<sup>23</sup> due to the reorientation of mobile water molecules, which is barely detectable as a small shoulder at  $\sim 90$  GHz, the upper frequency limit of the present spectra. In the previous study of NaCl(aq),<sup>19</sup> which was restricted to  $\nu \leq$

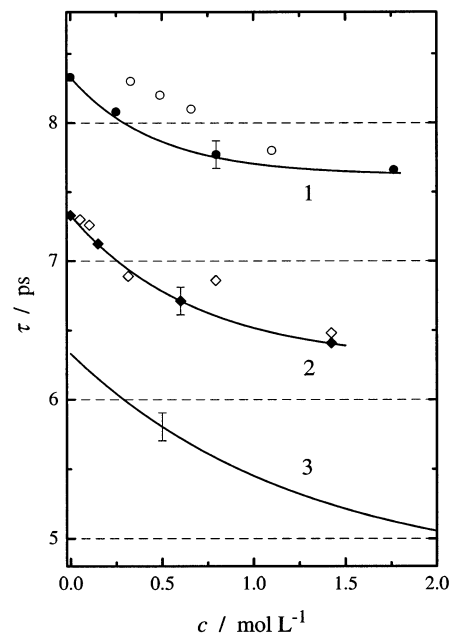


**Figure 4.** Dielectric relaxation times associated with the solvent,  $\tau$ , of aqueous solutions of CsCl (●) and KCl (◆, shifted by  $-1$  ps in  $\tau$ ) at 25 °C obtained from the full-range spectra of this work and compared with data from refs 25 (○) and 24 (◇). Also included are the fits of the data obtained with eq 4, curves 1 and 2, and the corresponding curve for NaCl (3, shifted by  $-2$  ps) obtained from the data of ref 19.

20 GHz, the high-frequency process could be ignored, and the spectra could be fitted with a Cole–Cole model using very small values of the distribution parameter  $\alpha$ . Even though the present measurements of KCl(aq) extend to 89 GHz, it was still not possible to define the high-frequency process because of the shift of the cooperative relaxation to higher frequencies with increasing electrolyte concentrations. Thus, a satisfactory fit for KCl(aq) was again obtained using the CC equation, with values of  $\alpha$  similar to those previously derived for NaCl(aq). For CsCl(aq), the data can also be fit with a CC model, but there were systematic, albeit minor, deviations at  $0.1 \leq c/M \leq 0.6$ . These will be discussed in detail in section 4.3.

**4.2. Relaxation Times.** The relaxation times ( $\tau$ ) for both KCl(aq) and CsCl(aq) were derived from the spectra measured over the full range of experimental frequencies. The  $\tau$  values so obtained (Figure 4) show decreases with increasing electrolyte concentration that are similar to those observed previously for NaCl(aq) and that can be fit by the exponential

$$\tau(c) = a \times \exp(-b \times c) + (\tau(0) - a) \quad (4)$$

where the relaxation time of pure water,  $\tau(0) = 8.33$  ps, was taken from ref 23. For KCl(aq), the present  $\tau$  values are in reasonable agreement with the somewhat scattered literature data<sup>24</sup> (Figure 4, curve 2). However, for CsCl(aq),<sup>25</sup> the agreement is only fair (Figure 4, curve 1). The present values are almost certainly more reliable because the  $\tau$  value reported by Wei et al.<sup>25</sup> for pure water is 8.5 ps, which is significantly larger than the  $(8.30 \pm 0.05)$  ps that is reported by others.<sup>17,23,26,27</sup> Approximately the same difference (0.2 ps) is observed for the salt solutions between the present values and those of Wei et al.<sup>25</sup>

The data in Figure 4 reveal that there are systematic differences in the shapes of the  $\tau$  versus  $c$  curves. These differences, expressed as the magnitude,  $a$ , and sensitivity,  $b$ , parameters in eq 4, are summarized in Table 3. Whereas  $a$  decreases in the order NaCl > KCl > CsCl,  $b$  increases. If it is

**TABLE 3: Parameters  $a$  and  $b$  of Equation 4 for the Concentration Dependence of the Bulk-Water Relaxation Time of Solutions of NaCl, KCl, and CsCl at 25 °C<sup>a</sup>**

electrolyte	$a$	$b$
NaCl <sup>b</sup>	$1.6 \pm 0.1$	$0.8 \pm 0.1$
KCl	$1.1 \pm 0.1$	$1.5 \pm 0.1$
CsCl	$0.7 \pm 0.1$	$2.1 \pm 0.5$

<sup>a</sup> Units:  $a$  in  $10^{-12}$ s;  $b$  in  $\text{L mol}^{-1}$ . <sup>b</sup> Input data from ref 19.

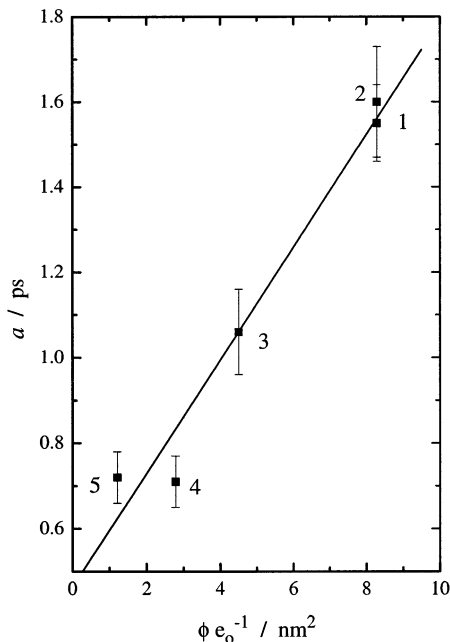


**Figure 5.** Magnitude parameter,  $a$ , of eq 4 as a function of the surface-charge density,  $\phi e_o^{-1}$ , of the cation for NaCl (1, ref 19), Na<sub>2</sub>SO<sub>4</sub> (2, ref 33), KCl (3), CsCl (4), and MgSO<sub>4</sub> (5, where  $r_+^{\text{eff}} = r_+ + 2r(\text{H}_2\text{O})$  (ref 31)).

assumed that the relaxation times of bulk water and the water in the hydration shell around Cl<sup>-</sup> (both of which are thought to be similarly fast, see discussion in ref 19) are independent of the electrolyte concentration, then these differences may arise from the increasing fragility of the coordination shell around the cation in going from Na<sup>+</sup> to Cs<sup>+</sup>.

Supporting evidence for such an effect is, however, not as clear cut as might be expected. Thus, X-ray and neutron diffraction data and computer simulations do show increasing M<sup>+</sup>-OH<sub>2</sub> distances<sup>11,28-39</sup> in going from Na<sup>+</sup> to Cs<sup>+</sup>. However, most of this increase is accounted for by the increase in the (crystallographic) radius of the cation, and only a small fraction can be ascribed to any real lengthening of the M<sup>+</sup>-OH<sub>2</sub> bond. However, the enthalpies of hydration of these ions,<sup>28</sup> which are dominated by the interactions in the first coordination shell, clearly indicate a decline in the M<sup>+</sup>-OH<sub>2</sub> bond strength from Na<sup>+</sup> through Cs<sup>+</sup>. Increasing coordination-shell fragility is certainly consistent with the molecular dynamics simulations of Chowdhuri and Chandra,<sup>30</sup> which suggest that the coordination number (CN) of NaCl(aq) decreases only from 5.55 to 5.32 over the concentration range of  $0 \leq c/M \leq 3.35$  whereas for KCl(aq) the decrease is from 7.40 to 6.60 over the same concentration range. Similarly, the present decrease in dielectric relaxation time in going from NaCl to CsCl is broadly consistent with the residence times in the primary hydration sphere calculated by Koneshan et al.<sup>29</sup>

Consistent with this evidence for the increasing fragility of the hydration sphere in going from Na<sup>+</sup> to Cs<sup>+</sup>, the magnitude of parameter  $a$  in eq 4 correlates reasonably well (Figure 5)

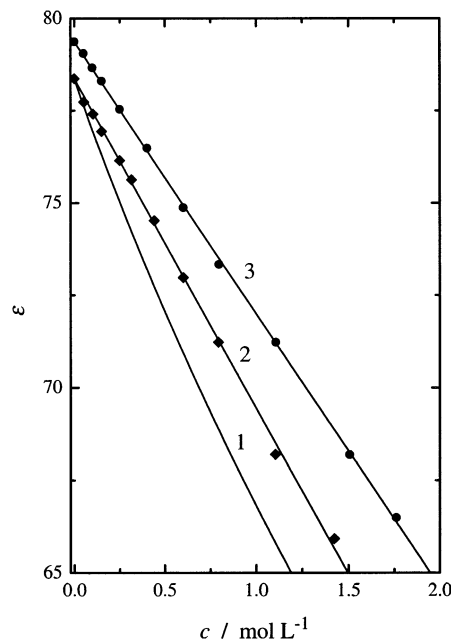


**Figure 6.** Static permittivity,  $\epsilon$ , of aqueous solutions of NaCl (curve 1, ref 19), KCl (2) and CsCl (3, shifted by +1 in  $\epsilon$ ) at 25 °C as obtained with the CC model.

with the cation surface-charge density  $\phi_i (= z_+ e_o / 4\pi r_+^2$ , where  $e_o$  is the elementary charge). Unfortunately, these results are too few for us to draw definitive conclusions: most of the published data are either of insufficient accuracy or appear to be affected by unresolved ion-pair contributions.<sup>17,32</sup> Also, it should be noted that, consistent with the presence of a very tightly bound first hydration shell that does not exchange on the DR time scale,<sup>11</sup> it is necessary to assume that the effective radius of Mg<sup>2+</sup>,  $r_+^{\text{eff}}$ , is  $(r_+ + 2r(\text{H}_2\text{O}))$  rather than the crystallographic radius  $r_+$  assumed for the other ions.

**4.3. Permittivities and Solvation Numbers.** Solvation numbers can be derived from DR data as described in detail elsewhere.<sup>19,33</sup> As for NaCl(aq), and as already noted, the data for KCl(aq) can be fit within the limits of experimental accuracy with a CC model. However, the permittivities so obtained show a linear decrease with electrolyte concentration (Figure 6, curve 2). In contrast, the permittivity of NaCl(aq),<sup>19</sup> and indeed of most other strong electrolytes in water and other solvents,<sup>17,33</sup> is a curved function of concentration (Figure 6, curve 1). The solvent permittivities for CsCl(aq) obtained from a CC fit are almost identical to those of KCl(aq) except that they have a somewhat smaller slope when plotted against  $c$  (Figure 6, curve 3,  $\epsilon$  values shifted by +1 for clarity).

The magnitudes of the slope (strictly, the initial slopes) of these curves, the so-called “dielectric decrements”, are opposite to what would be expected on the basis of the cation sizes (Figure 6; see also Figure 9). In principle, such a sequence can be explained by a decrease in  $Z_{\text{IB}}$ , the number of “irrotationally bound” (IB) water molecules (effectively those water molecules that are “frozen” on the DR time scale), in going from Na<sup>+</sup> to Cs<sup>+</sup>.

The values of  $Z_{\text{IB}}$  can be obtained as

$$Z_{\text{IB}} = \frac{c_s^o - c_s^{\text{ap}}}{c} \quad (5)$$

where  $c_s^o$  is the analytical concentration of the solvent,  $c$  is the electrolyte concentration, and  $c_s^{\text{ap}}$  is the number of (rotation-

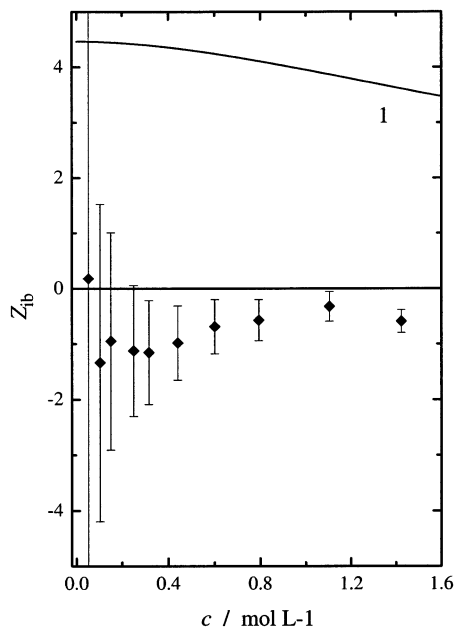


**Figure 7.** Number of irrotationally bound water molecules per equivalent of electrolyte,  $Z_{IB}$  ( $\blacklozenge$ ), as a function of electrolyte concentration,  $c$ , for KCl(aq) at 25 °C assuming slip boundary conditions for kinetic depolarization. Curve 1 indicates the corresponding NaCl data.<sup>19</sup> The error bars represent an assumed error of 0.5% in  $\epsilon$ .

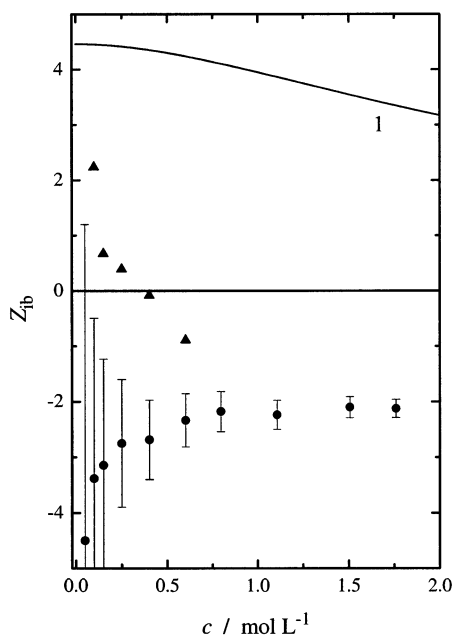


**Figure 8.** Number of irrotationally bound water molecules per equivalent of electrolyte,  $Z_{IB}$ , as a function of electrolyte concentration,  $c$ , for CsCl(aq) at 25 °C assuming slip boundary conditions for kinetic depolarization: CC model ( $\bullet$ ), 2D model ( $\blacktriangle$ ). Curve 1 indicates the corresponding NaCl data.<sup>19</sup> The error bars represent an assumed error of 0.5 in  $\epsilon$  and are similar for the 2D model.

ally) “free” solvent molecules, which is calculated from the Cavell equation<sup>32,36</sup> normalized with respect to the pure solvent

$$c_s^{ap} = \frac{2\epsilon(c) + 1}{2\epsilon(0) + 1} \cdot \frac{\epsilon(0)}{\epsilon(c)} \cdot \frac{(1 - \alpha_s f_s(c))^2}{(1 - \alpha_s f_s(0))^2} \cdot \frac{c_s^0(0)}{S_s(0)} \cdot S_s(c) \quad (6)$$

In eq 6,  $\alpha_s$  is the polarizability, and  $f_s$  is the reaction field factor of water.

Correcting for the kinetic depolarization of the ions assuming slip boundary conditions for ion transport, which has been shown

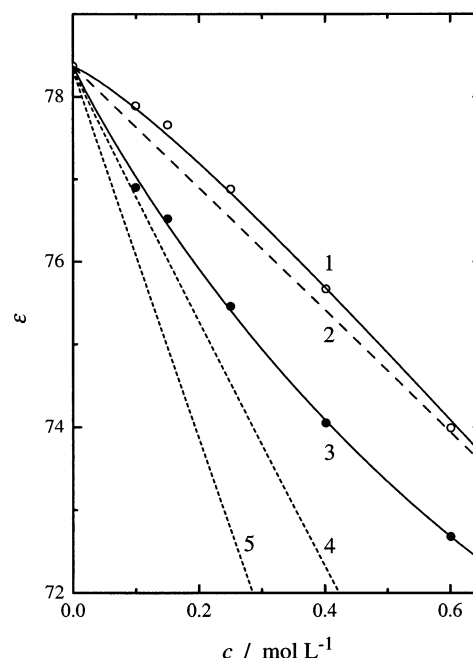


**Figure 9.** Static permittivity of the solutions ( $\epsilon$ , curve 1) and of water ( $\epsilon_2$ , curve 3) in CsCl(aq) according to the 2D model and the solution permittivity obtained for the CC model (curve 2). Also indicated are the water permittivities,  $\epsilon_2$ , in aqueous Me<sub>4</sub>NBr (curve 4) and Et<sub>4</sub>NBr (curve 5) solutions.<sup>34</sup>

elsewhere to yield a consistent series of  $Z_{IB}$  values for various ions,<sup>19,22</sup> produces for KCl the  $Z_{IB}$  values plotted in Figure 7. Further assuming that all of the IB water is associated with the cations (i.e.,  $Z_{IB}(\text{Cl}^-) = 0$ ), the data in Figure 7 show that there is indeed a decrease from  $Z_{IB}(\text{Na}^+) \approx 4$  to  $Z_{IB}(\text{K}^+) \approx 0$  within the rather large error limits. Such a difference accounts for KCl(aq) having a smaller dielectric decrement than NaCl(aq). The values of  $Z_{IB}(\text{K}^+) \approx Z_{IB}(\text{Cl}^-) = 0$  are also consistent with the linearity of the  $\epsilon$  versus  $c$  plot for KCl. Similar near-linear  $\epsilon$  versus  $c$  plots have also been observed for R<sub>4</sub>NX(aq)<sup>34</sup> and nonionic solutes<sup>35</sup> where the number of water molecules frozen out of the bulk by the solute is essentially zero.

An explanation of the smaller dielectric decrement for CsCl(aq) is more complex. As already noted, the CsCl(aq) data can be fit with a Cole–Cole model. However, a combination of the permittivities so obtained with the Cavell equation results in physically unrealistic negative values of  $Z_{IB}$  (Figure 8). Thus, it appears that the CC model may not be fully appropriate for the DR of CsCl(aq), and an explanation of the smaller dielectric decrement of CsCl(aq) must lie elsewhere. Again, as noted above, there are small but systematic deviations from the CC plot at low CsCl concentrations. At higher concentrations ( $c > 0.6\text{M}$ ), such differences are swamped out by the conductivity contribution ( $\nu_{\min}$  increases, Figure 2a). If the data at  $c \leq 0.6\text{M}$  are processed separately, then a better fit is obtained by assuming a two-Debye-process (2D) model (Table 2) with the second small relaxation process being centered on  $\sim 1.5\text{GHz}$  (Figure 3). This second process is most reasonably ascribed to the formation of a weak ion pair. Appropriately subtracting its contribution to the total permittivity produces lower values for the solvent permittivity (compare curves 2 and 3 in Figure 9) and results in a dielectric decrement for CsCl(aq) that is larger than that for KCl(aq), consistent with the cation sizes. Furthermore, although the errors are rather large at low concentrations, an estimation of the  $Z_{IB}$  values using the solvent permittivities derived from the 2D model and eqs 5 and 6, again assuming kinetic depolarization of the ions under slip boundary conditions,

gives  $Z_{\text{IB}}(\text{Cs}^+) \approx 0$  (Figure 8). This is both physically realistic and broadly consistent with the data for NaCl(aq) and KCl(aq) discussed above (Figure 7).

**4.4. Possible Ion Pairing in CsCl(aq).** The possibility of ion-pair formation in CsCl(aq) noted above appears at first glance to contradict conventional wisdom about ion association. This view, embodied, for example, in the Bjerrum equation and the Born model of electrostatic interactions,<sup>14,28</sup> predicts that association should *decrease* with increasing ionic size. Such effects are well established for many systems<sup>37,38</sup> and have been widely assumed in many other areas of chemistry.<sup>39,40</sup> However, a considerable body of evidence suggests that other factors are also in operation. Although such effects may be somewhat weaker than typical electrostatic interactions, they may nevertheless have significant consequences.

As long ago as 1974, Pethybridge and Spiers<sup>41</sup> showed that, with sufficient care in processing the data, the very weak ion association detected in simple 1:1 electrolytes by high-quality conductivity measurements *increased* with increasing ionic size. This was attributed by them<sup>41</sup> to the increasing likelihood of larger ions colliding with each other but might also be related to increasing polarizability (covalency) or solvent-structure breaking effects. Recent simulation studies<sup>29</sup> have suggested that two types of hydration occur for the alkali metal cations, which the authors termed electrostatic (hydrophilic) ion solvation and cage formation (hydrophobic hydration). The former predominates with the smaller cations whereas the latter becomes important for the larger cations, resulting, for example, in a maximum in the solvation entropies as a function of ion size.<sup>29,42</sup> Circumstantial evidence for greater-than-expected binding of simple ligands by  $\text{Cs}^+$  has also been obtained by Raman studies.<sup>43,44</sup> In particular, it was postulated that the extent of contact ion-pair (CIP) formation increased with increasing cation size as a result of the decreasing strength of the (primary) hydration sphere.<sup>44</sup> This can occur even if the overall formation constant shows the opposite trend. Finally, the possibility of ion pairing in CsCl(aq) has also been invoked by Fawcett and Tikanen<sup>45</sup> to explain departures of observed activity coefficients from those calculated using a mean spherical approximation model.

If ion pairing is assumed to be responsible for the low-frequency process in CsCl(aq), then, using the procedures outlined in detail previously,<sup>33</sup> the association constants shown in Figure 10 are obtained via the 2D model, with ion radii and polarizabilities taken from Marcus.<sup>46</sup> Two sets of data are given, one corresponding to the formation of a CIP and the other, to a singly solvent-separated ion pair (SIP). For convenience, both sets of values were fit to a Guggenheim-type equation<sup>1</sup>

$$\log \beta = \log K_{\text{A}} - \frac{2A_{\text{DH}}|z_+z_-|\sqrt{I}}{1 + \sqrt{I}} + b_{\beta}I \quad (7)$$

with  $K_{\text{A}}$  and  $b_{\beta}$  as adjustable parameters.  $A_{\text{DH}} = 0.5110 \text{ dm}^3/2 \text{ mol}^{-1/2}$  for water at 25 °C, and  $I = 1/2 \sum c_i z_i^2 = c - c_{\text{IP}}$  is the ionic strength.

On the basis of their conductivity measurements, Paterson et al.<sup>47</sup> derived a  $K_{\text{A}}$  value of 0.49 for CsCl(aq). The numerical values of such small association constants are highly dependent on the accuracy of the data and the type of conductance equation adopted for the analysis. (Pethybridge and Spiers<sup>41</sup> give  $K_{\text{A}} \approx 0.5$ .) Nevertheless, the estimates of  $K_{\text{A}}$  using either an SIP or a CIP model are very much larger, with  $K_{\text{A}} = 9.5 \pm 0.3$  for CIP and  $2.7 \pm 0.1$  assuming SIP.

The  $K_{\text{A}}$  value derived from the CIP model (Figure 10, curve 1) is chemically unlikely and clearly inconsistent with the

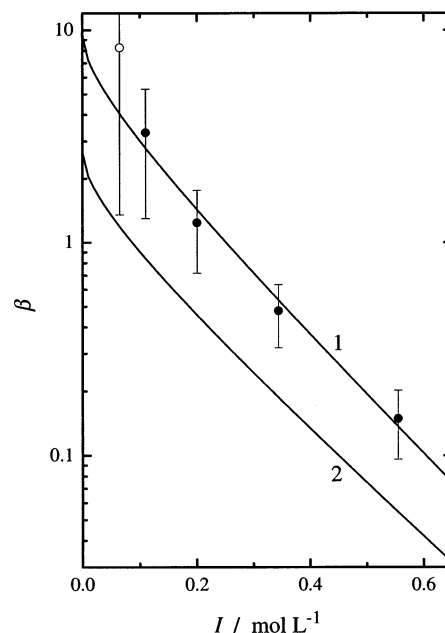


**Figure 10.** Stability constants,  $\beta$ , as a function of ionic strength,  $I$ : (●) calculated from the ion-pair amplitude  $\epsilon - \epsilon_2$  of the 2D model assuming CIP and fit with eq 7, curve 1. If SIP are assumed (data not shown), then curve 2 is obtained with eq 7. The error bars represent an assumed error of 0.5% in  $\epsilon$  and  $\epsilon_2$ ; (○) datum not fit.

conductivity data. The  $K_{\text{A}}$  value derived from the SIP model (Figure 10, curve 2) *seems* more realistic and is closer to the conductivity result. The relaxation time of the lower-frequency process,  $\sim 140$  ps, is more consistent with an SIP than a CIP, for which a relaxation time of  $\sim 30$  ps would be expected on the basis of the Stokes–Einstein–Debye equation.<sup>48</sup> Nevertheless, the detailed analysis of the DR data given above and the insights provided by the simulation studies<sup>29,30</sup> suggest that it is *not* physically reasonable to propose that SIPs form to any significant extent in CsCl(aq) solutions. A double solvent-separated ion pair (2SIP) would predict an even lower  $K_{\text{A}}$  value that would be more consistent with the conductivity data; however, such a species would need to be stable on the time scale of a few hundred picoseconds.<sup>49</sup> This would be inconsistent with both the DR observations and the simulations.

A credible explanation of this discrepancy is the existence of small systematic errors in the present data. Although within the likely error limits, the systematic decrease of  $Z_{\text{IB}}$  from positive to negative values for the 2D model ( $\blacktriangle$  points in Figure 8) suggests indeed some “overcompensation” at low  $c$ . Given the very small magnitude of the observed effects (Figures 3 and 9) and the restricted range of concentrations for which any effect could be observed before being swamped by the conductivity contribution (see section 4.3), this would not be surprising. All that can be said confidently about the present data is that there is evidence for weak ion pairing in CsCl(aq) but there is insufficient reliable information to determine its strength or type. In this context, the association constant determined from the high-precision conductivity analyses<sup>41,47</sup> should be regarded as more meaningful than the present estimates.

It is of interest to investigate related salts such as RbCl and the corresponding (Cs and Rb) bromides and iodides because their aqueous solutions are believed to be more highly associated than CsCl(aq).<sup>45,50</sup> However, this was beyond the scope of the present study, and in view of the present results, such investigations should be postponed until the accuracy of DRS is improved

by at least a factor of 3. For the CIPs of these salts, that of CsI would have the largest dipole moment,  $\mu_{IP} \approx 30$  D. With  $K_A = 0.56$ ,<sup>50</sup> ion-pair dispersion amplitudes  $S_1 = \epsilon - \epsilon_2 \lesssim 0.8$  would be expected.  $S_1$  values for the other salts and also for CsCl at other temperatures should be similar or even smaller. As for the present data for CsCl(aq) at 25 °C, such values of  $S_1$  are (at best) close to our experimental resolution, and although the presence of ion pairs would probably be detected, similar ambiguities in the interpretation of the data would probably be encountered.

**Acknowledgment.** We thank W. Kunz for enabling the interferometer measurements and for his hospitality during the stay of T.C. in his laboratory.

**Supporting Information Available:** Tables of the complex permittivity data as a function of frequency for the investigated KCl and CsCl solutions. This material is available free of charge via the Internet at <http://pubs.acs.org>.

## References and Notes

- (1) Robinson, R. A.; Stokes, R. H. *Electrolyte Solutions*, 2nd ed.; Butterworth: London, 1970.
- (2) Harned, H. S.; Owen, B. B. *The Physical Chemistry of Electrolyte Solutions*, 3rd ed.; Reinhold: New York, 1957.
- (3) *Activity Coefficients in Electrolyte Solutions*, 2nd ed.; Pitzer, K. S., Ed.; CRC Press: Boca Raton, FL, 1991.
- (4) *The Chemical Physics of Solvation*; Dogonadze, R. R., Kálmán, E., Kornyshev, A. A., Ulstrup, J., Eds.; Elsevier: Amsterdam, 1986; Part B.
- (5) *Stability Constants of Metal-Ion Complexes*; Sillen, L. G., Martell, A. E., Eds.; Chemical Society: London, 1964, 1971; Special Publications 17 and 25.
- (6) Capewell, S. G.; Hefter, G. T.; May, P. M. *Talanta* **1999**, *49*, 25.
- (7) Kratsis, S.; Hefter, G. T.; May, P. M. *J. Solution Chem.* **2001**, *30*, 19.
- (8) *Properties of Aqueous Solutions of Electrolytes*; Zaytsev, I. D., Aseyev, G. G., Eds.; CRC Press: Boca Raton, FL, 1992.
- (9) Lobo, V. M. M.; Quaresma, J. L. *Electrolyte Solutions: Literature Data on Thermodynamic and Transport Properties*; University of Coimbra Chemistry Department: Coimbra, Portugal, 1982 and 1984; Vols. 1 and 2.
- (10) *CRC Handbook of Chemistry and Physics*, 76th ed.; Lide, D. R., Ed.; CRC Press: Boca Raton, FL, 1995.
- (11) Ohtaki, H.; Radnai, T. *Chem. Rev.* **1993**, *93*, 1157.
- (12) Böttcher, C. F. J.; Bordewijk, P. *Theory of Electric Polarization*, 2nd ed.; Elsevier: Amsterdam, 1978; Vol. 2.
- (13) Scaife, B. K. P. *Principles of Dielectrics*; Clarendon: Oxford, 1989.
- (14) Barthel, J.; Krienke, H.; Kunz, W. *Physical Chemistry of Electrolyte Solutions*; Steinkopff/Springer: Darmstadt/New York, 1998.
- (15) Barthel, J.; Buchner, R.; Eberspächer, P.-N.; Münsterer, M.; Stauber, J.; Wurm, B. *J. Mol. Liq.* **1998**, *78*, 82.
- (16) Buchner, R.; Barthel, J. *Annu. Rep. Prog. Chem. C* **2001**, *97*, 349.
- (17) Barthel, J.; Buchner, R.; Münsterer, M. *Electrolyte Data Collection, Part 2: Dielectric Properties of Water and Aqueous Electrolyte Solutions*; Kreysa, G., Ed.; Chemistry Data Series; DECHEMA: Frankfurt, 1995; Vol. 12.
- (18) Pottel, R. In *Water, A Comprehensive Treatise*; Franks, F., Ed.; Plenum Press: New York 1973; Vol. 3, Chapter 8.
- (19) Buchner, R.; Hefter, G. T.; May, P. M. *J. Phys. Chem. A* **1999**, *103*, 1.
- (20) Barthel, J.; Popp, H. *J. Chem. Inf. Comput. Sci.* **1991**, *31*, 107. Electrolyte DATA Regensburg is a subset of the database DETHERM; Distributor: STN, Karlsruhe, Germany.
- (21) Barthel, J.; Bachhuber, K.; Buchner, R.; Hetzenauer, H.; Kleebauer, M. *Ber. Bunsen-Ges. Phys. Chem.* **1991**, *95*, 853.
- (22) Buchner, R.; Hefter, G. T.; May, P. M.; Sipos, P. *J. Phys. Chem. B* **1999**, *103*, 11186.
- (23) Buchner, R.; Barthel, J.; Stauber, J. *Chem. Phys. Lett.* **1999**, *306*, 57.
- (24) Popp, K.-H. Ph.D. Thesis, Universität Regensburg, Regensburg, Germany 1987. Data are tabulated in ref 17.
- (25) Wei, Y. Z.; Chiang, P.; Sridhar, S. *J. Chem. Phys.* **1992**, *96*, 4569.
- (26) Kaatze, U. *J. Chem. Eng. Data* **1989**, *34*, 371.
- (27) Ellison, W. J.; Lamkaouchi, K.; Moreau, J.-M. *J. Mol. Liq.* **1996**, *68*, 171.
- (28) Marcus, Y. *Ion Solvation*; Wiley: New York, 1985.
- (29) Koneshan, S.; Rasaiah, J. C.; Lynden-Bell, R. M.; Lee, S. H. *J. Phys. Chem. B* **1998**, *102*, 4193.
- (30) Chowdhury, S.; Chandra, A. *J. Chem. Phys.* **2001**, *115*, 3732.
- (31) Buchner, R.; Chen, T.; Hefter, G. *J. Phys. Chem. B*, submitted for publication.
- (32) Barthel, J.; Hetzenauer, H.; Buchner, R. *Ber. Bunsen-Ges. Phys. Chem.* **1992**, *96*, 1424.
- (33) Buchner, R.; Capewell, S. G.; Hefter, G. T.; May, P. M. *J. Phys. Chem. B* **1999**, *103*, 1185.
- (34) Buchner, R.; Hölzl, C.; Stauber, J.; Barthel, J. *Phys. Chem. Chem. Phys.* **2002**, *4*, 2169.
- (35) Kaatze, U. *J. Solution Chem.* **1997**, *26*, 1049.
- (36) Cavell, E. A. S.; Knight, P. C.; Sheikh, M. A. *J. Chem. Soc., Faraday Trans.* **1971**, *67*, 2225.
- (37) Baes, C. F.; Mesmer, R. E. *The Hydrolysis of Cations*; Wiley: New York, 1976.
- (38) Hefter, G. T. *Coord. Chem. Rev.* **1974**, *12*, 221 and references therein.
- (39) See, for example, Atkinson, G.; Kor, S. K. *J. Phys. Chem.* **1967**, *71*, 673.
- (40) See, for example, Barthel, J.; Wachter, R.; Gores, H.-J. In *Modern Aspects of Electrochemistry*; Conway, B. E., Bockris, J. O'M., Eds.; Plenum Press: New York, 1979; Vol. 13, Chapter 1.
- (41) Pethybridge, A.; Spiers, D. J. *J.C.S. Chem. Commun.* **1974**, 423.
- (42) Lynden-Bell, R. M.; Rasaiah, J. C. *J. Chem. Phys.* **1997**, *107*, 1981.
- (43) Kratsis, S.; Hefter, G. T.; May, P. M.; Sipos, P. *Aust. J. Chem.* **2000**, *53*, 363.
- (44) Sipos, P.; Bolden, L.; Hefter, G. T.; May, P. M. *Aust. J. Chem.* **2000**, *53*, 887.
- (45) Fawcett, W. R.; Tikanen, A. C. *J. Phys. Chem.* **1996**, *100*, 4251.
- (46) Marcus, Y. *Ion Properties*; Marcel Dekker: New York, 1997.
- (47) Paterson, R.; Jalota, S. K.; Dunsmore, H. S. *J. Chem. Soc. A* **1971**, 2116.
- (48) Dote, J. L.; Kivelson, D.; Schwartz, R. N. *J. Phys. Chem.* **1981**, *85*, 2169.
- (49) Buchner, R.; Barthel, J. *J. Mol. Liq.* **1995**, *63*, 55.
- (50) Tikanen, A. C.; Fawcett, W. R. *Ber. Bunsen-Ges. Phys. Chem.* **1996**, *100*, 643.